Title

Hypolimnetic deoxygenation enhanced production and export of recalcitrant dissolved organic matter in a large stratified reservoir

Authors

Qu, Liyin
He, Chen
Wu, Zetao
et al.

Publication Date

2022-07-01

DOI

10.1016/j.watres.2022.118537

Peer reviewed

Water Research 219 (2022) 118537

Contents lists available at ScienceDirect

Water Research

journal homepage: www.elsevier.com/locate/watres

Hypolimnetic deoxygenation enhanced production and export of recalcitrant dissolved organic matter in a large stratified reservoir

Liyin Qu [a,b], Chen He [c], Zetao Wu [b], Randy A. Dahlgren [d], Mingxing Ren [a,b], Penghui Li [e], Quan Shi [c], Yan Li [f], Nengwang Chen [a,b,f,*], Weidong Guo [a,b,f,*]

[a] State Key Laboratory of Marine Environmental Science, College of Ocean and Earth Sciences, Xiamen University, Xiamen 361012, China
[b] Fujian Provincial Key Laboratory for Coastal Ecology and Environmental Studies, Xiamen University, Xiamen 361012, China
[c] State Key Laboratory of Heavy Oil Processing, China University of Petroleum, Changping District, Beijing 102249, China
[d] Department of Land, Air and Water Resources, University of California, Davis 95616, USA
[e] School of Marine Sciences, Sun Yat-sen University, Zhuhai 519082, China
[f] National Observation and Research Station for the Taiwan Strait Marine Ecosystem, Xiamen University, Xiamen 361012, China

ARTICLE INFO

Keywords:
Dissolved organic matter
Stratified reservoir
Hypolimnetic deoxygenation
Carbon transformation
Optical analysis
FT-ICR MS

ABSTRACT

Global impoundment of river systems represents a major anthropogenic forcing to carbon cycling in reservoirs with seasonal thermal stratification. Currently, a quantitative and mechanistic understanding of how hypolimnetic deoxygenation in stratified reservoirs alters dissolved organic matter (DOM) cycling and lateral transport along the river continuum remains unresolved. Herein, we used optical and high-resolution mass spectrometric analyses to track seasonal and spatial compositional changes of DOM from a large, subtropical impounded river in southeast China. Aliphatic compounds were contributed by algal blooms to epilimnetic DOM during the spring/summer and by baseflow to the overall DOM pool during low-discharge periods. Deoxygenation-driven hypolimnetic mineralization enhanced in situ production of bio-refractory molecules and humic-like fluorescent DOM ($FDOM_H$) by utilizing bio-labile DOM and settling biogenic particles during periods of stratification. Production efficiency of hypolimnetic $FDOM_H$ was 159–444% higher than that of the global dark ocean, and was strongly regulated by temperature and possibly substrate supply. The in situ production rate of hypolimnetic $FDOM_H$ was four to five orders-of-magnitude higher than the dark ocean, with much faster turnover rates in dark inland waters versus the dark ocean. Collectively, these findings indicate that the hypolimnion is a hotspot for microbial carbon transformations, and hence an important source and pool of refractory DOM in aquatic systems. The lateral $FDOM_H$ flux increased 10.8–32.1% due to hypolimnetic reservoir release during periods of stratification, highlighting the importance of incorporating hypolimnetic carbon transformations into models for carbon cycling of inland waters and the land-sea interface.

1. Introduction

Export of dissolved organic matter (DOM) from land to sea represents an important linkage between terrestrial and oceanic carbon pools, with an estimated flux of ~250 Tg C yr^{-1} (Raymond and Spencer, 2015). However, this linkage has been greatly altered by widespread river impoundment, as only 23% of global long rivers (> 1000 km) maintain free connectivity to the sea (Grill et al., 2019). The building of more than 58,000 global dams with heights over 15 m has enhanced primary productivity in the epilimnion of reservoirs, thereby increasing contributions of autochthonous DOM, which is considered relatively bio-labile (Zhou et al., 2021). Further, the longer water residence time substantially promotes in-reservoir microbial degradation of labile DOM, whether the source is in-situ produced or externally supplied (Maavara et al., 2017). The degradation of settling biogenic particles in water column and sediments could also contribute to the DOM pool, especially to the bio-refractory DOM (RDOM) pool (Thottathil et al., 2013; Yang et al., 2014; Attermeyer et al., 2018). These active processes have inevitably altered the composition and bioavailability of DOM released to downstream rivers and ultimately to the sea (Thottathil et al., 2013), further modulating carbon transformations and ecological functions of estuarine and coastal environments (Yu et al., 2021; Regnier et al.,

* Corresponding author at: State Key Laboratory of Marine Environmental Science, College of Ocean and Earth Sciences, Xiamen University, Xiamen 361012, China.
E-mail addresses: nwchen@xmu.edu.cn (N. Chen), wdguo@xmu.edu.cn (W. Guo).

https://doi.org/10.1016/j.watres.2022.118537
Received 13 January 2022; Received in revised form 29 April 2022; Accepted 29 April 2022
Available online 2 May 2022

2022). To date, an integrated evaluation of how these processes change properties and export flux of fluvial DOM across the reservoir-river continuum remains largely unexplored.

The hypolimnion usually occupies a dominant volume of medium to large reservoirs/lakes having relatively deep depths (Han et al., 2018; Yi et al., 2021). Notably, there is consistent hypolimnetic oxygen consumption (i.e. deoxygenation) during seasonal thermal stratification periods (Thottathil et al., 2013; Jane et al., 2021), accompanied by strong mineralization (i.e., release of CO_2 and nutrients) (Thottathil et al., 2013; Yan et al., 2021). Previous studies found that deoxygenation-driven mineralization in the hypolimnion of Lake Biwa and the dark ocean was closely related to microbial degradation of bio-labile particulate organic matter (POM) and DOM substrates and the associated production of bio-refractory humic-like fluorescent DOM ($FDOM_H$) (Thottathil et al., 2013; Wang et al., 2021a). Higher temperature and a greater supply of labile substrates could enhance these microbial degradation/production processes (Wang et al., 2021a). However, hypolimnetic DOM cycling in reservoirs has received little attention compared with epilimnetic waters (Wang et al., 2021b).

Reservoirs often have an abundant input of labile substrates, relatively long duration of stratification and a high percentage volume of hypolimnetic deoxygenation waters (Yan et al., 2021; Yi et al., 2021). The hypolimnetic temperature of reservoirs are generally higher than the dark ocean at the same latitudes (Wang et al., 2021a). Thus, we assume that deoxygenation in the hypolimnion of stratified reservoirs could play a key role in regulating microbial transformations of fluvial DOM. In particular, the transformed DOM components could be directly exported from reservoirs through the hypolimnetic release point to downstream river segments. Therefore, the hypolimnion of reservoirs is critical in regulating the quality and reactivity of fluvial DOM along the reservoir-river continuum. However, factors regulating hypolimnetic DOM transformations and its lateral transport are still unknown.

Fluvial DOM is a complex mixture of organic molecules that challenges the suitability and interpretability of various characterization techniques. Many studies found that $FDOM_H$ could be used as a quantitative tracer for RDOM production due to its strong correlation with apparent oxygen utilization (AOU) in dark inland and ocean waters (Yamashita and Tanoue, 2008; Thottathil et al., 2013; Wang et al., 2021a). The $FDOM_H$ per unit oxygen consumption slope can thus be used to estimate in situ production efficiencies in the hypolimnion of reservoirs. Once oxygen utilization rates are available, the in situ production rates and turnover time of hypolimnetic $FDOM_H$ can be quantified (Catalá et al., 2015; Wang et al., 2021a). Therefore, excitation-emission matrices (EEMs) from fluorescence spectroscopy, which reveal information on the source and biogeochemical reactivity of both DOM and base-extracted fluorescent POM (FPOM) (Lee et al., 2018; Qu et al., 2021), are valuable tools to understand the deoxygenation-related seasonal dynamics of organic matter in reservoir-river systems.

Ultrahigh-resolution Fourier transform ion cyclotron resonance mass spectrometry (FT-ICR MS), which can identify thousands of DOM molecular formulas and specific compounds (Kellerman et al., 2018; Koch and Dittmar, 2016), provides another powerful tool to trace deoxygenation-related degradation and transformation of DOM (Martínez-Pérez et al., 2017; Wang et al., 2021b). For example, the degradation index (I_{DEG}) of DOM was determined to be related to AOU in the deep northeast Atlantic Ocean (Hansman et al., 2015). Similarly, molar ratios (e.g., O/C, N/C) provide additional evidence to trace the accumulation of O-rich compounds and removal of N-moieties via microbial processing (Osterholz et al., 2021). Therefore, the combination of optical and mass spectroscopy techniques provides complementary benefits to explore organic matter cycling in dynamic river-reservoir systems.

The Min River is the third largest river by runoff that flows into the marginal China Sea. Shuikou (SK) reservoir, impounding the main stem of the lower Min River, is the largest subtropical reservoir in southeast China. The limnology of the reservoir shows a typical seasonal stratification-overturn cycle and notable hypolimnetic deoxygenation (Yan et al., 2021), which is similar to other subtropical or temperate reservoirs/lakes (Thottathil et al., 2013; Han et al., 2018; Xu et al., 2021). The dam site for SK reservoir is just 50 km upstream of the tidal excursion in the macrotidal Min Estuary during dry seasons. Thus, any transformation in DOM quantity/quality within the reservoir can quickly flow through the short distance to the East China Sea. Therefore, SK reservoir provides an ideal site to study the effects of river-reservoir regulation on organic matter transformations and its influence on DOM transport along the river continuum.

Herein, we performed optical and high-resolution mass spectrometric analyses of DOM from vertical water columns in SK reservoir and along the river-reservoir continuum (i.e., upstream – reservoir [epilimnion/hypolimnion] – downstream) in the four seasons and a spring-flood event of 2020–21. Our objectives were to: (1) investigate sources and vertical variations of DOM and POM properties within the reservoir on a seasonal timescale; (2) trace deoxygenation-driven hypolimnetic DOM transformation, especially the production rate and turnover time of hypolimnetic $FDOM_H$ and its regulating factors; and (3) quantify the alteration of lateral DOC, POC and $FDOM_H$ fluxes by reservoir hypolimnetic regulation and export along the river continuum.

2. Materials and methods

2.1. Study area

The Min River watershed (60,992 km^2) is located in a subtropical monsoon climate zone of southeast China (116°23′–119°35′E, 25°23′–28°16′N). Mean annual temperature is 16–20 °C and the multi-year (1950–2010) average precipitation and runoff are 1700 mm and 6.2×10^{10} m^3, respectively. About 70–80% of the precipitation and runoff occurs between April and September (Yan et al., 2021), with the largest monthly precipitation in May/June often accompanied by late-spring flood events. Land cover is dominated by forest (73.1%), agricultural (18.9%) and urban (4.6%) lands. Soils are predominantly organic-poor red soil and lateritic red soil.

Shuikou reservoir, completed in 1996, is a mildly eutrophic system with an area of ~94 km^2 (Yan et al., 2021). The drainage area upstream of the dam accounts for 86% of the total Min River watershed. Water storage ($1.8–1.9 \times 10^9$ m^3) and water level (59.8 ± 1.3 m) were relatively stable during the June 2020 - June 2021 sampling period (Fig. S1). The water residence time (WRT) in summer and late-spring flood periods was estimated as 12.7 ± 7.8 days (mean ± std dev) and 6.8 ± 1.7 days, respectively, which was significantly shorter than autumn (33.4 ± 14.4 days), winter (47.8 ± 1.6 days) and non-flood spring (33.3 ± 3.5 days) periods (Fig. 1). Impounded water is usually exported from the hypolimnetic release point (~30 m depth), whereas epilimnetic release occurs only during flood events.

2.2. Sampling campaign

Five investigations were performed in summer (July 2020), autumn (November 2020), winter (January 2021), spring (April 2021) and for a spring-flood event (May 2021) (Fig. 1). Surface water samples were collected by Niskin bottles at the upstream river (U1), reservoir (R1-R7) and downstream river (D1-D5) sites. High-resolution vertical sampling (0.5, 2, 5, 10, 20, 30, 40 and 50 m) was conducted at reservoir sites of R1, R4 and R7, which displayed generally consistent vertical profile variations (Yan et al., 2021). All samples were analyzed for DOC, POC, FDOM, FPOM and nutrients. Samples for FT-ICR MS analysis were only collected at sites of U1, R4 (0.5, 30 and 50 m) and D5. Additionally, four similar vertical sampling events for FDOM analyses were previously performed at three reservoir sites (R1, R4 and R7) in summer (August 2017), autumn (November 2017) and winter (January 2018) and early autumn (2019).

Water samples were filtered immediately after sampling through 0.7

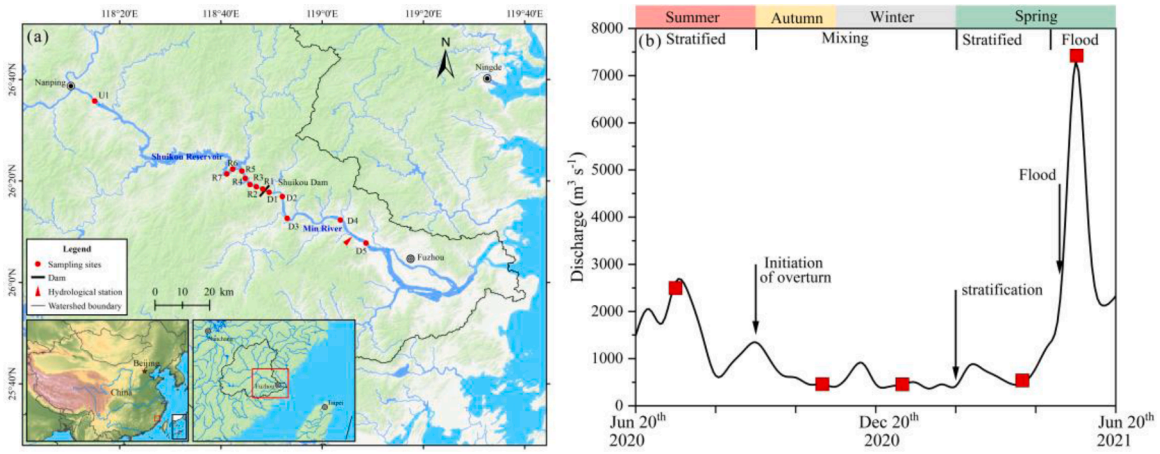

Fig. 1. Sampling map (a) and ten-day average discharge of the Min River at the D5 location during the sampling period (b, red squares indicate the detailed sampling dates). The D5 site is near (~0.6 km) a principle hydrological station (Zhuqi) for the Min River.

μm, pre-combusted (500 °C, 10 h) GF/F filters (Whatman, UK). Filtrates for DOC (acidified to pH = 2), FDOM and nutrient analyses were stored at 4 °C and analyzed within one week of collection. Solid-phase extraction of filtrates for FT-ICR MS (acidified to pH = 2) was also pretreated within one week of collection. Particles retained on the GF/F filters were used for FPOM analysis. To reduce filter background C-contamination, samples for POC analysis were filtered through 2.2 μm, pre-combusted (650 °C, 10 h) quartz filters (Whatman, UK) (Qu et al., 2021). The filters for FPOM and POC were stored at −20 °C before analysis.

Temperature (± 0.01 °C), Chl *a* (± 0.1 μg/L) and DO (± 0.1 mg/L) profiles at R1, R4 and R7 sites were performed using a calibrated YSI Multiparameter Water Quality Sonde (Xylem, USA). Calibration of the DO sensor was based on measurements of discrete water samples using the Winkler method (Yan et al., 2021). The relative water column stability (RWCS), the index used to depict the stratification condition of reservoirs, was calculated as follows (Wang et al., 2021b):

$$\mathrm{RWCS} = \frac{\rho_b - \rho_w}{\rho_4 - \rho_5} \quad (1)$$

Where ρ_b and ρ_w represent density of bottom water and density at a given depth, respectively. The ρ_4 and ρ_5 parameters are water density at 4 °C and 5 °C, respectively.

2.3. Measurements of DOC, POC and nutrients

DOC concentrations were determined using a TOC-L analyzer (Shimadzu, Japan) with triplicates (± 2%, analytical error). POC filters were firstly acidified with 2 M HCl (Merck, Germany) to remove inorganic carbon; POC was then determined using a Multiwavelength Thermal/Optical Carbon Analyzer (DRI, USA) with duplicates (± 5%, analytical error). Nitrate (NO_3–N) and soluble-reactive phosphate (SRP) concentrations were measured with an AA3 Auto-Analyzer (SEAL, Germany) with duplicates (± 5%, analytical error).

2.4. FT-ICR MS analysis of DOM

A 500-mL aliquot of filtered DOM sample was extracted by solid-phase extraction (SPE) using 500-mg Agilent Bond Elut PPL cartridges (Dittmar et al., 2008) (Text S2). The PPL cartridges were eluted with ~7 mL methanol (Merck, Germany). Recovery efficiencies for SPE-DOM ranged from 40.3% to 69.5% (57.1 ± 8%), consistent with typical recovery rates (50–60%) using similar DOM SPE methodologies (Dittmar et al., 2008; Wang et al., 2021b). Extracts of SPE-DOM were analyzed using a 9.4 Apex-ultra X FT-ICR MS (State Key Laboratory of Heavy Oil Processing, China University of Petroleum) under negative mode (128 scans) with an electrospray ionization source (Bruker Apollo II). All analytical processes and instrument settings followed the methodology of He et al. (2020a). Mass peaks ranged from 200 to 800 *m/z* with a signal/noise ratio (S/N) > 6 and detection error of < 1 ppm. Detected elemental formulas were bound within the constraints of $C_{1–60}$, $H_{1–120}$, $N_{0–3}$, $O_{0–30}$ and $S_{0–1}$ (He et al., 2020a).

The degradation index (I_{DEG}) was calculated following Flerus et al. (2012). The compound categories of SPE-DOM were defined following Kellerman et al. (2018) based on the modified aromaticity index (AI_{mod}) and H/C ratio (Koch and Dittmar, 2016): condensed aromatic (CA, AI_{mod} > 0.66), polyphenols (Poly, 0.66 ≥ AI_{mod} > 0.5), highly unsaturated compounds (HU, AI_{mod} < 0.5 and H/C < 1.5), unsaturated aliphatic compounds (UA, 2 ≥ H/C ≥ 1.5, $N = 0$) and peptides (2 ≥ H/C ≥ 1.5, $N > 0$). The CA+Poly components are characterized as bio-refractory DOM from allochthonous sources or produced via humification processes, whereas the UA+Peptides are generally autochthonous bio-labile DOM components (Kellerman et al., 2018). The HU-associated materials may include terrestrially-source components and polyphenol-peptide reaction products (Hockaday et al., 2009).

2.5. Optical analyses of FDOM and FPOM

FFPOM filters were extracted using 10 mL of 0.1 M NaOH for 24 h in dark at 4 °C (Qu et al., 2021). Extracted solutions were pH-neutralized and filtered through 0.22 μm polyethersulfone filters for subsequent fluorescence analysis. The excitation-emission matrix spectra (EEMs) of FDOM and FPOM were measured with a −7100 fluorescence spectrophotometer (Hitachi, Japan) following the procedures of Wang et al. (2021a) and Qu et al. (2021). Samples with high absorbance were pre-diluted to avoid perturbations from inner filter effects. The fluorescence intensity of base-extractable FPOM samples was corrected for the volumes of extraction solution and filtered water samples (Qu et al., 2021).

Two humic-like components and three protein-like components were identified using a total of 349 EEMs and the PARAFAC model with DOMfluor toolbox 1.7 and validated by split-half analysis (Fig. S2) (Stedmon and Bro, 2008). The C1 and C4 components were selected to represent the typical humic-like ($FDOM_H$/$FPOM_H$) and protein-like components ($FDOM_P$/$FPOM_P$), respectively (Text S1). Spearman rank correlation showed that the molecules (2408) associated with $FDOM_H$ had a higher percentage of CA+Poly (12.9–22.7%) than $FDOM_P$ (1.8–5.2%), and the molecules (3146) associated with $FDOM_P$ had a higher percentage of UA+Peptides (8.6–23.8%) than $FDOM_H$ (0.7–0.9%) ($p < 0.05$, Fig. S3; Table S1). Therefore, the $FDOM_H$ in SK reservoir was mainly composed of bio-refractory materials, whereas the

$FDOM_P$ fraction was more bio-labile in nature.

2.6. Net flux variations for DOC, POC and FDOM due to reservoir regulation

To assess the net flux variations for DOC, POC and FDOM due to river regulation by SK reservoir, a simple box model considering the difference between the input flux and export flux of the reservoir was used:

$$F_{Net} = (C_D - C_U) \times Q \quad (2)$$

Where C_D and C_U are average values of DOC, POC and FDOM in the downstream river and upstream river, respectively. Q is the fluvial discharge of the Min River.

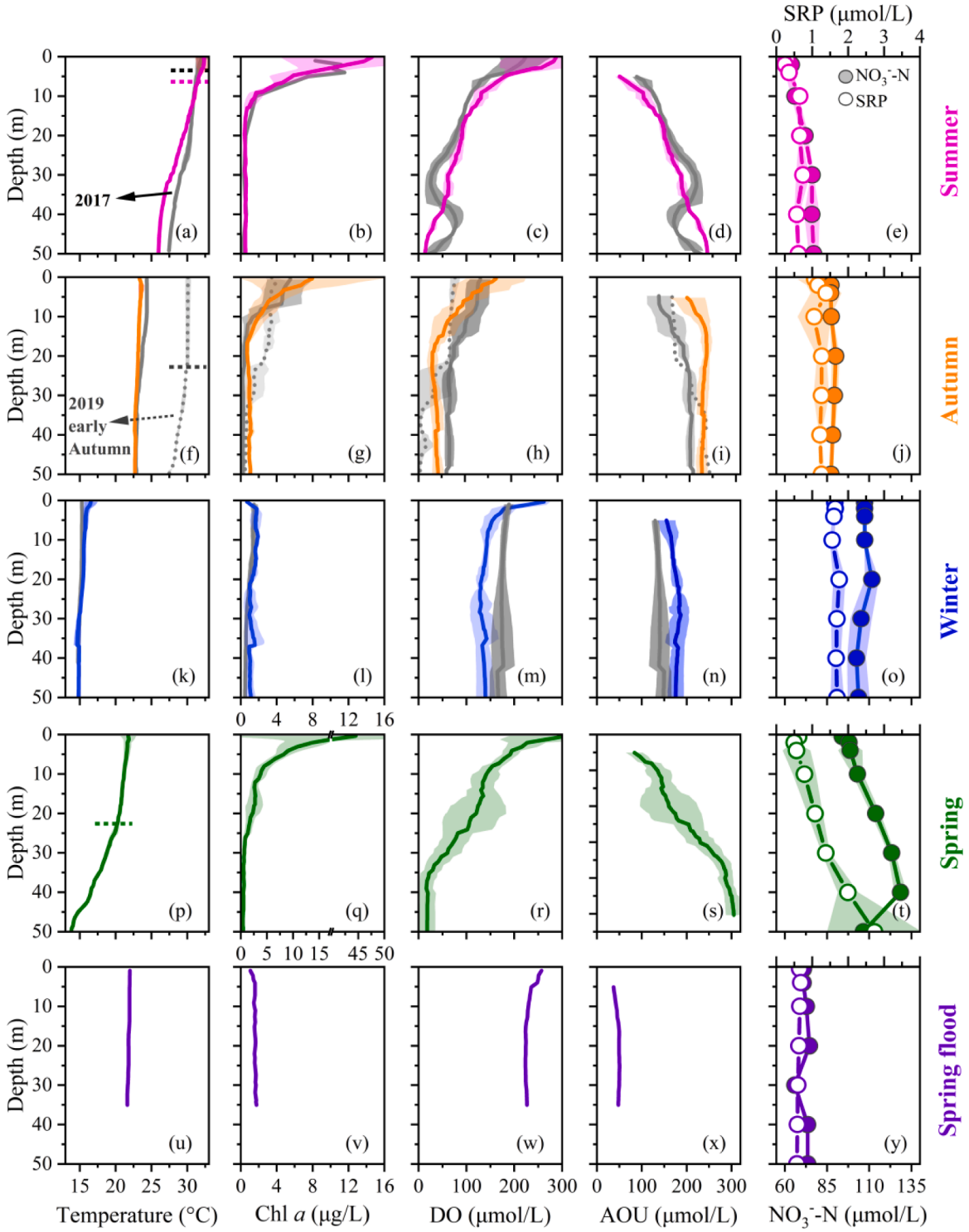

Fig. 2. Vertical profiles of temperature, Chl *a*, DO, AOU, NO_3—N and SRP during different seasons of 2020–21 in SK reservoir. Color band represents error bars comprising the three sites (R1, R4 and R7). grey solid and dotted lines represent data from a preliminary investigation in 2017–18 and early autumn of 2019, respectively.

2.7. In situ production rates and turnover times for hypolimnetic $FDOM_h$ in SK reservoir

In situ production rates for $FDOM_H$ (PR, QSU d^{-1}) in the hypolimnion of SK reservoir, an optical tracer of RDOM, was quantified as follows (Wang et al., 2021a):

$$PR = PE \times OUR \quad (3)$$

Where PE (QSU (μmol L^{-1}) $^{-1}$) is in situ production efficiencies of $FDOM_H$, i.e. the slope between $FDOM_H$ and AOU. OUR (μmol kg^{-1} d^{-1}) is the oxygen utilization rate, which is defined as the average oxygen consumption magnitude of the hypolimnion during the water residence time.

The turnover time for $FDOM_H$ (T, d^{-1}) in SK reservoir was defined as the time required to produce the net hypolimnetic $FDOM_H$ inventory from in situ production rate:

$$T = \frac{(C_D - C_U)}{PR} \quad (4)$$

2.8. Data analysis

SPSS 22.0 was used for all statistical analyses (IBM, USA). Figures were generated using ArcGIS 10.2 (Esri, USA) and Origin 2021b (OriginLab, USA).

3. Results

3.1. Water column vertical profiles of temperature, Chl a, oxygen and nutrients

Vertical temperature profiles at three reservoir stations showed little difference among sites, but similar seasonal variations (Fig. 2). Thermal stratification was well developed in summers and spring (Fig. 2a, p), except for the flood period (Fig. 2u). The temperature differences during the stratification period (4–8 °C) were significantly lower than for other stratified reservoirs (e.g. Hongjiadu, 16 °C) or lakes (e.g. Lake Biwa, 20 °C) with longer water residence times (172–753 d) ($p < 0.05$) (Thottathil et al., 2013; Yi et al., 2021). However, the high stratification indices (RWCS) indicate that the stratification conditions in SK reservoir were notably pronounced (Fig. S4). Well-mixing of the upper layer during early autumn deepened the thermocline (> 20 m), which marked initiation of the overturn process (Fig. S4b). Thereafter, thermal stratification was absent in autumn and winter when northeast monsoon-driven water mixing was prevalent (Fig. 2f, k).

Chl *a* (0.2–102.8 μg/L) showed large seasonal variations (Fig. 2). Epilimnetic algae blooms (Chl *a* > 10 μg/L) were observed during spring and summers (Fig. 2b, q). The Chl *a* decreased in autumn and reached its lowest level in winter (Fig. 2g, l), but was also very low during the late-spring flood period (Fig. 2v). Further, Chl *a* showed relatively high values in the 10–30 m layer in early autumn due to vertical overturning (Fig. 2g).

Epilimnetic DO concentrations were generally saturated/supersaturated when Chl *a* was high in spring and summer (Fig. 2c, r). The overturn of low DO water during the monsoon transition period decreased the surface DO in autumn (Fig. 2h). Conversely, hypolimnetic DO during the summer, autumn and spring reached hypoxic or even anoxic status, with AOU (> 5 m depth) increasing with depth and reaching its highest levels in deeper layers (Fig. 2d, i, s). DO replenishment occurred throughout the entire water column during winter and the late-spring flood period when the vertical temperature gradient was small (Fig. 2m, w).

Nitrate and SRP ranged from 52.1 to 131.1 μmol/L and 0.23–3.67 μmol/L, respectively, with the highest concentrations in spring and winter (Fig. 2o, t). Both nutrients increased with depth in spring and summer (Fig. 2e, t), whereas they showed only small vertical variations in autumn, winter and the spring-flood period (Fig. 2j, o, y).

3.2. Water column vertical profiles of DOM and POM parameters

3.2.1. DOC and FDOM

DOC and bio-labile protein-like $FDOM_P$ ranged from 85.8 to 197 μmol/L and 0.07–0.28 RU (Fig. 3), and showed strong correlations in summer, winter and spring (r: 0.65–0.89; $p < 0.05$). During the spring and summer period of stratification, both DOC and $FDOM_P$ profiles significantly decreased from the surface to the bottom of the water column ($p < 0.05$) (Figs. 3 and 4a, c). Conversely, $FDOM_P$ showed only a small vertical variation in early autumn, but displayed a consistent increase with depth in autumn and winter. The $FDOM_P$ profile during the spring-flood period and DOC profiles in autumn/winter showed little vertical variation.

The bio-refractory humic-like $FDOM_H$ (0.23–0.37 RU) generally showed an opposite water column profile to that of DOC during the stratified period and reached its highest levels in the hypolimnion in the summers of 2017 and 2020 ($p < 0.05$; Figs. 3b and 4e). $FDOM_H$ was also high during the spring-flood period with little vertical variation. Moreover, $FDOM_H$ showed a slight increase with depth in autumn compared to a decreasing tendency in winter when the lowest values were observed.

3.2.2. Molecular composition of SPE-DOM

FT-ICR MS parameters exhibited significant seasonal variations in their molecular composition ($p < 0.05$) (Fig. 3 and Table S2). During summer, the vertical profiles of bio-refractory CA+Poly, HU compounds and I_{DEG} indices generally increased from the epilimnion to the deep layer, but CA+Poly slightly decreased in the deep layer (Figs. 3d, 3e and 4g, i, j). In contrast, the bio-labile UA+Peptides sharply decreased with depth (Fig. 4h). The molecular difference comparison showed that there was a 58% increase of CA+Poly and 87% decrease of UA+Peptides in the hypolimnion. The strong correlation between CA+Poly with $FDOM_H$ or between UA+Peptides with $FDOM_P$ suggested that the vertical variation of molecular compounds between the epilimnion and hypolimnion should also be significant.

During autumn, the CA+Poly compounds and I_{DEG} remained at a relatively high level and showed a general decrease in the hypolimnion, whereas the HU compounds and UA+Peptides compounds slightly increased (Fig. 3i, j and 4 g, j), accompanied by a 57% increase of formulas with high H/C (> 1.5) in the hypolimnion. During winter and spring, the CA+Poly compounds and I_{DEG} throughout the water column were significantly ($p < 0.05$) lower than in summer and autumn, whereas UA+Peptides showed the opposite tendency (Figs. 3 and 4g, h, j). The HU compounds showed a slight increase in the deep layer during winter, while it decreased with depth in spring (Fig. 4i).

3.2.3. POC and FPOM

POC, $FPOM_P$ and $FPOM_H$ ranged from 12.2 to 423 μmol/L, 0.001–0.067 RU and 0–0.11 RU, respectively (Fig. 3). The POC and FPOM parameters showed higher average values in spring/summer than autumn/winter ($p < 0.05$). In spring and summer, the POC and FPOM parameters were correlated (r: 0.66–0.77; $p < 0.05$), and all parameters quickly decreased in the 0–10 m layer and showed significantly lower values in the hypolimnion ($p < 0.05$) (Fig. 4). There was a weak decrease in the vertical magnitude of POC, $FPOM_P$ and $FPOM_H$ concentrations in autumn, and all parameters became well-mixed in winter. Notably, all three parameters increased with depth during the spring-flood period.

3.3. Variations of DOM and POM parameters along the river-reservoir continuum

3.3.1. DOC and FDOM

Along the river continuum, DOC and $FDOM_P$ increased during summer and spring from the upstream river to the reservoir epilimnion,

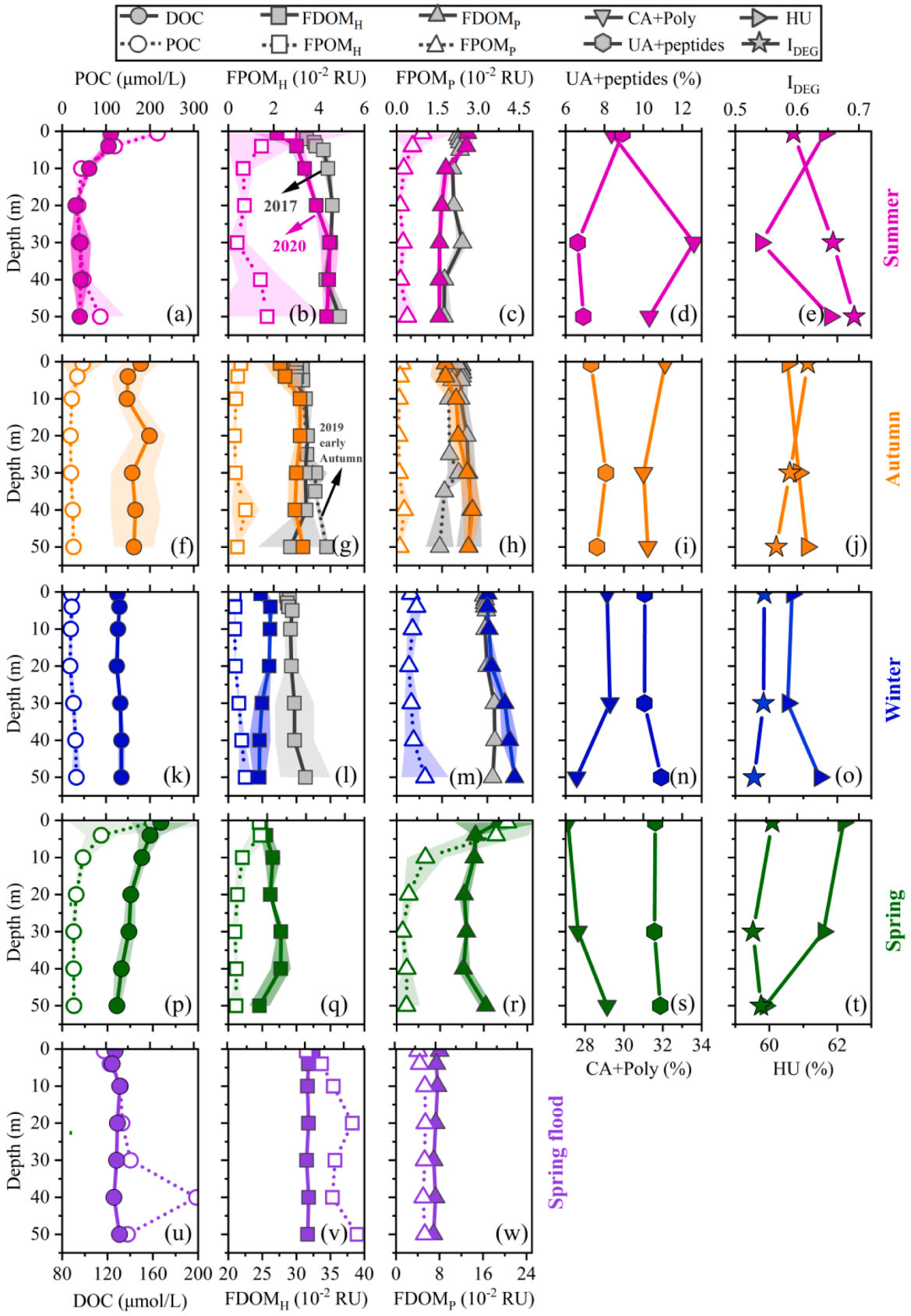

Fig. 3. Water column vertical profiles for carbon concentration, optical and molecular parameters of DOM (color solid lines) and POM (color dotted lines) in SK reservoir during 2020–2021. grey lines in second and third columns are data from a preliminary investigation of humic-like and protein-like FDOM ($FDOM_H$ and $FDOM_P$) in 2017–18 and early autumn of 2019, respectively.

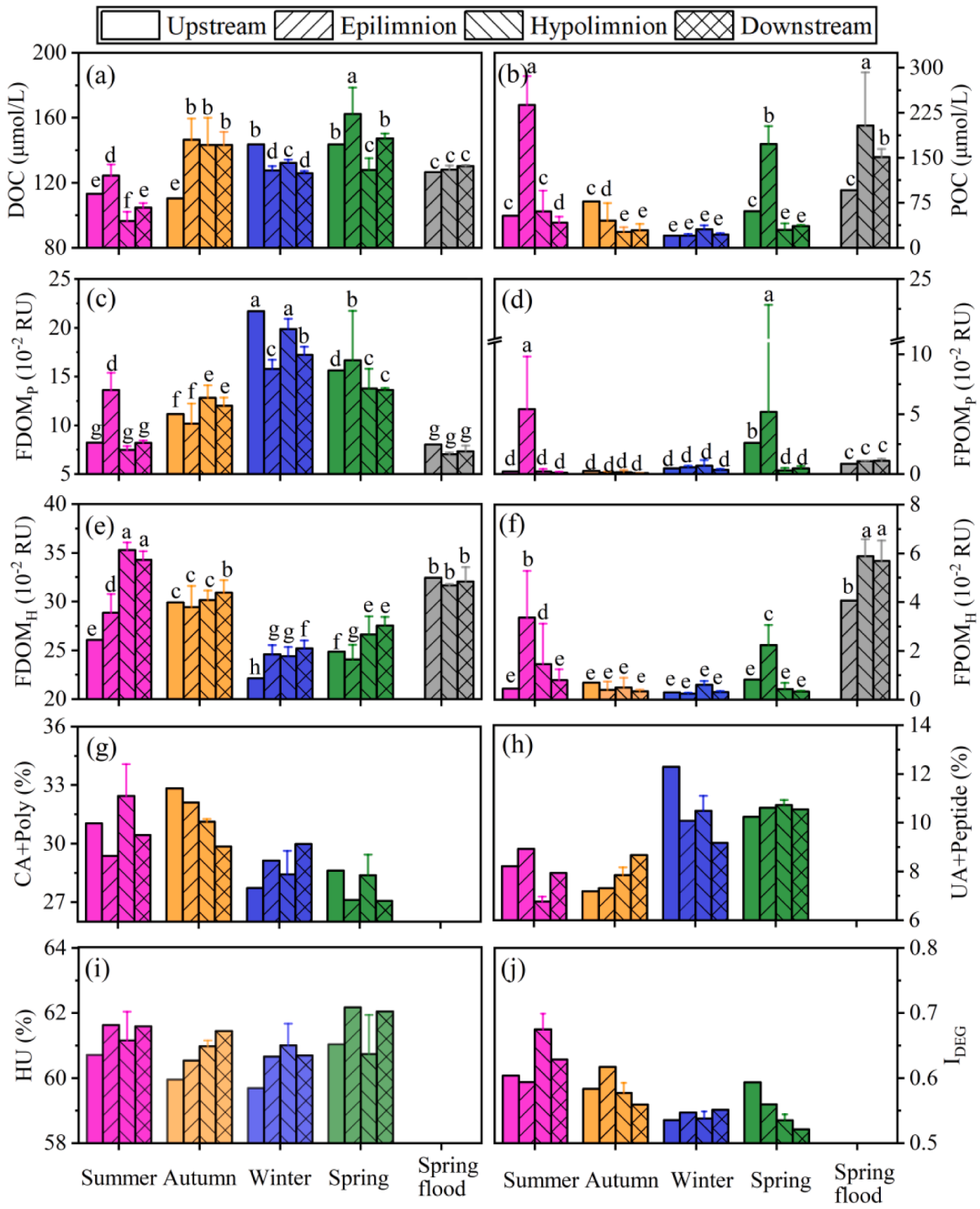

Fig. 4. Variation of optical and chemical parameters of DOM/POM along the river continuum in different seasons. Note: Bars with different letters indicate a significant difference at $p < 0.05$.

but decreased in the downstream river (Fig. 4a, c). In contrast, DOC and $FDOM_P$ generally increased from upstream to downstream in autumn, whereas both parameters decreased along the continuum in winter. During the spring-flood period, both parameters showed similar values in the epilimnion and downstream river. $FDOM_H$ generally increased along the continuum during summer, winter and spring, but showed little variation in autumn and the spring-flood period (Fig. 4e).

3.3.2. *Molecular composition of SPE-DOM*

Summer values for CA+Poly compounds and I_{DEG} decreased from the upstream river to the epilimnion of the reservoir, but increased in the downstream river (Fig. 4g, j). These parameters generally decreased from the upstream river to downstream river during autumn, while consistently increasing during winter. During spring, CA+Poly compounds decreased from the upstream river to the epilimnion with only small variations in the downstream river, whereas I_{DEG} showed a continuous decrease. UA+Peptides compounds generally showed an opposite trend to that of CA+Poly compounds during all seasons (Fig. 4h). HU compounds generally showed an increasing trend along the continuum during all seasons (Fig. 4i).

3.3.3. POC and FPOM

The POC and $FPOM_P$/$FPOM_H$ sharply increased from the upstream river to the epilimnion followed by a decrease in the downstream river during summer and spring (Fig. 4b, d, f). In autumn, POC continuously decreased along the continuum, but the FPOM parameters showed only small variations. The POC and FPOM parameters showed only small lateral variations during winter and the spring-flood period.

3.3.4. Alteration of lateral organic matter fluxes by reservoir regulation

The annual lateral flux of bio-refractory $FDOM_H$ showed an increase of 9.6 ± 0.7% after passage through SK reservoir (Table S3). This increase was much higher in the stratified summer period (32.1%) than in other seasons (3.4–14.5%). Conversely, annual lateral fluxes of DOC and bio-active $FDOM_P$ showed slight decreases (0.4 ± 0.7% and 5.1 ± 1.2%) due to reservoir regulation (Table S3). The decrease in the annual POC flux along the river continuum was much larger (15.9 ± 5.7%) than for DOC and $FDOM_P$. On the seasonal timescale, the DOC flux showed an increase in spring and autumn, in contrast to a decrease in summer and winter. Except for a slight increase in autumn, the $FDOM_P$ flux showed a decrease in all other seasons. The decrease in the POC flux (22.9−61.8%) occurred for all seasons except winter. There was little variation of lateral DOC and FDOM fluxes during the spring-flood event, although the event DOC flux value (i.e., ~40% of the annual flux) was quite large and there was an obvious increase in the event POC flux (i.e., ~66% of the annual flux).

4. Discussion

4.1. Sources and transformations of epilimnetic DOM in SK reservoir

There were several significant seasonal variations in sources of epilimnetic DOM and its transformations along the river-reservoir-river continuum. During the wet summer season, DOC concentrations in the upper river were low (~110 μmol/L) compared with Arctic (1028 ± 21 μmol/L; Cory et al., 2015), USA rivers with extensive wetlands (390 ± 172 μmol/L; Spencer et al., 2013; Bhattacharya and Osburn, 2020), and other Chinese rivers (e.g., Changjiang, 144 ± 24 μmol/L; Jiulong River, 161 ± 21 μmol/L; Guo et al., 2014). We ascribe these lower DOC concentrations to limited DOC flushing and dilution effects from the organic-poor soils of the SK watershed (Liu et al., 2019). DOC and bio-labile $FDOM_P$ increased from the upper river to the epilimnion of the reservoir (Fig. 4a, c), suggesting an in situ contribution from algal blooms (Fig. 2b, q) (Yi et al., 2021). This process was accompanied by production of degradable POM (Fig. 4b, d), which provides sufficient biogenic substrates with a C/N mass ratio of 5.8 to support microbial deoxygenation and mineralization after settling to the hypolimnion (Yan et al., 2021). The increase of $FDOM_H$ and HU compounds indicates that terrestrial inputs also contribute to the epilimnetic DOM pool (Fig. 4e, i) (He et al., 2021b). However, the CA+Poly components showed a decreasing tendency (Fig. 4g), which may reflect selective degradation of the photo-labile fraction of terrestrial DOM under reduced flow velocity and correspondingly higher WRTs (Stubbins et al., 2010).

In spring, the sampling period with the highest dominance of base flow, the DOC and bio-labile signals in the reservoir epilimnion showed a similar autochthonous contribution as in summer, but values were much higher in the upstream river (Fig. 4a, c, h). This may result from groundwater contributions, which have an enrichment of aliphatic components (Kellerman et al., 2018; Wagner et al., 2019), and both high DOC and bio-labile signals during the low-flow season (Hong et al., 2012). In autumn, there was little variation for optical properties, but an increase of epilimnetic DOC and HU compounds across the continuum (Fig. 4a, i). These results suggest a contribution of non-fluorescent DOM to the epilimnetic carbon pool (Pereira et al., 2014). This non-fluorescent DOM (mainly HU compounds) could be derived from the input of degradation products from terrestrial plants (e.g. highly oxidized tannins) (Hockaday et al., 2009; Huber et al., 2011), which are not correlated with FDOM components (Fig. S3). In winter, a base flow dominated hydrologic period, significantly higher $FDOM_P$ and UA+Peptides were observed in the upper river than during summer and autumn ($p < 0.05$). These bio-labile compounds decreased in the epilimnion along with a simultaneous increase of bio-refractory compounds (Fig. 4g, h) indicating microbial transformation of DOM along the continuum (He et al., 2020b; Oliver et al., 2016).

4.2. Deoxygenation enhanced production of recalcitrant DOM in the hypolimnion

In the hypolimnion of the stratified SK reservoir, bio-refractory $FDOM_H$, inorganic nutrients (NO_3–N and SRP) and dissolved inorganic carbon (DIC, unpublished data) increased with depth and showed a strong positive correlation with AOU (r: 0.54–0.87; $p < 0.05$) (Fig. 5a). These trends were accompanied by an increase of CA+Poly compounds (Fig. 3). The linear correlation between hypolimnetic $FDOM_H$ and AOU remained through initiation of the overturn in early autumn (r: 0.88; $p < 0.05$). Conversely, DOC and bio-labile $FDOM_P$ decreased with depth and showed a negative correlation with AOU (r: −0.49 to −0.69; $p < 0.05$; Fig. 3 and 5b). The profiles for UA+Peptides, POC and biogenic $FPOM_P$ also decreased with depth (Fig. 3). Collectively, these patterns can be attributed to in situ production of RDOM components at the expense of bio-labile dissolved and particulate organic substrates during microbial deoxygenation-related mineralization in the stratified hypolimnion (Ogawa et al., 2001; Zhou et al., 2021; Wang et al., 2021a). This process, which is similar to the "microbial carbon pump" hypothesis for the deep ocean (Jiao et al., 2018), can be summarized as:

$$\text{Bio}-\text{labile DOM} \Big/ \text{POM} + \text{O}_2 \xrightarrow[\text{deoxygenation}]{\text{microbes}} \underset{\text{(mineralization)}}{\text{Nutrients (N, P)}} + \text{DIC} + \underset{\text{(transformation)}}{\text{RDOM}} \quad (5)$$

Our previous in situ incubation experiment in SK reservoir also showed that hypolimnetic microbial respiration of organic matter was the major contributor to oxygen consumption (96.5–99.9%) during the stratified summer period (Yan et al., 2021). Additionally, microbial activity in porewaters of the upper sediment column may enhance accumulation of RDOM (e.g. CA+Poly and CRAMs) due to degradation of both allochthonous and autochthonous bio-labile organic matter substrates (Zhou et al., 2022). Production of bio-refractory $FDOM_H$ by anaerobic respiration in deeper sediments may occur during early diagenesis (Chen et al., 2017). These RDOM components could be released to the overlying water from the sediment-water interface under low oxygen conditions (Yang et al., 2014). The relative contribution of water column production versus sediment production to the hypolimnetic RDOM pool remains an important question requiring further study.

Difference between hypolimnetic and epilimnetic molecular formulas revealed the molecular features of degraded or produced DOM during hypolimnetic mineralization (Fig. 6). During the stratified summer period, the degraded UA+Peptides fraction included CHO, CHON and CHOS compounds with a high H/C ratio (> 1.5) (Fig. 6a-c). There was also selective microbial degradation of the heteroatomic CHOS and CHONS compounds (i.e., N- or S-containing HU and polyphenol compounds) with a low H/C ratio (< 1.5) (Fig. 6c, d). The hypolimnetic-produced RDOM components were enriched in HU compounds containing a high percentage (75%) of carboxyl-rich alicyclic molecules (CRAMs) (Fig. 6a-d), especially for CHO compounds. The abundant CHON compounds (45.4%) in the hypolimnetic CA+Poly fraction infers possible microbial production of bio-refractory N-containing formulas (Fig. 6b) (Wagner et al., 2015). The molecular variation during the stratified spring period is similar to the summer (Fig. 6m, n), but with much less degradation of heteroatomic CHOS and CHONS compounds

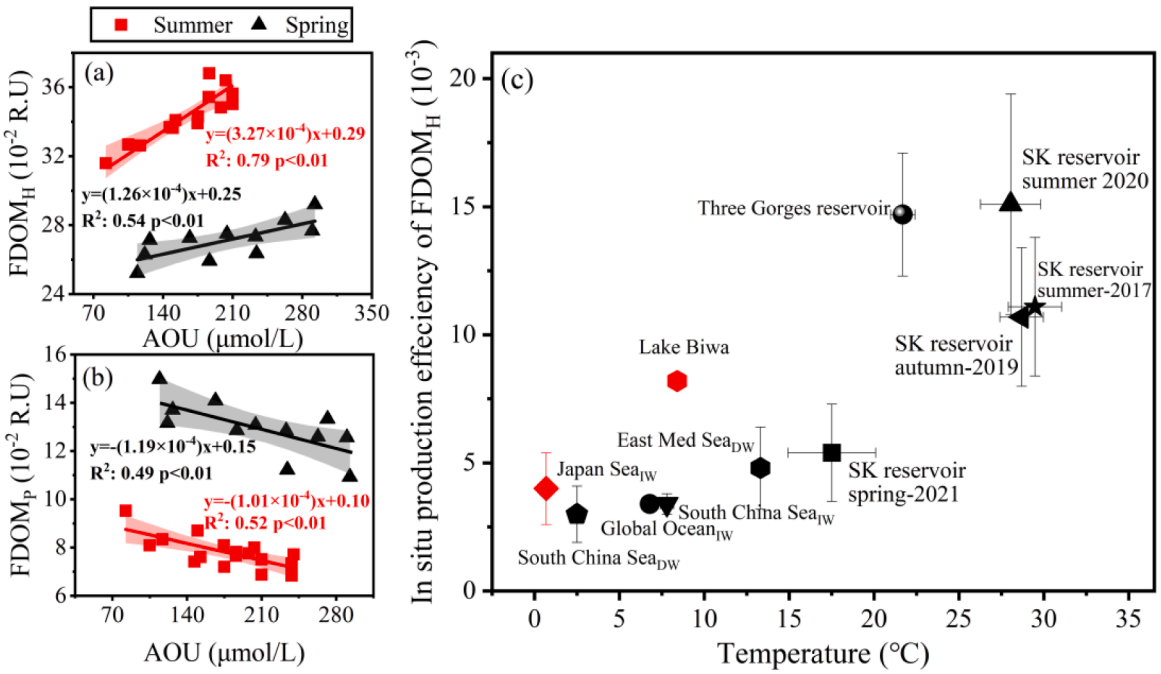

Fig. 5. Relationships between $FDOM_H$ (a) and $FDOM_p$ (b) with AOU in SK reservoir, and a comparison of the relationship between in situ $FDOM_H$ production efficiency and temperature across inland and marine systems (c). Note that $FDOM_H$ in panel (c) is expressed with fluorescence intensity of peak M (Ex/Em = 290–325/370–430 nm) for consistency with the literature (Thottathil et al., 2013; Wang et al., 2021a).

(Fig. 6o, p), which is consistent with limited microbial production of RDOM (Fig. 3q, s) in spring.

The in situ specific production efficiency of $FDOM_H$ per unit oxygen consumption in the hypolimnion of SK reservoir during the warmer summer was appreciably higher than that of the colder spring season, as well as in the temperate, stratified Lake Biwa (central Japan) (Fig. 5c). These limited results suggested a strong temperature regulation for the specific production efficiency of $FDOM_H$ components in inland dark waters, as previously demonstrated for global dark marginal basins (Wang et al., 2021a). Thus, the temperature regulation of deoxygenation-related microbial production of RDOM components could be a widespread phenomenon in stratified freshwater systems similar to that found for marine dark systems.

The shorter WRT in summers (12.7 ± 7.8 days) than in spring (33.3 ± 3.5 days) for the stratified SK reservoir resulted in only a small decrease in summer hypolimnetic temperature (28.3 ± 1.9 °C). This relatively 'high' temperature environment enhances summer hypolimnetic microbial activity, thereby facilitating higher OUR (Table 1) and in situ production efficiency of $FDOM_H$ compared to the cooler spring (Smale et al., 2017; Mao and Li, 2018) (Fig. 5c). As a result, there was a much higher net in situ production rate for hypolimnetic $FDOM_H$, and a corresponding 32.1% increase of $FDOM_H$ export flux in summer than in spring (10.8%). This occurred in spite of the higher hypolimnetic AOU during the spring with a longer WRT versus summers with a shorter WRT (Fig. 2d, s). This could also be the case for other reservoirs (e.g., Three Gorges reservoir) in tropical and subtropical areas experiencing wet and warm summer periods of stratification (Wang et al., 2021b). Therefore, variation in reservoir WRTs during periods of stratification may influence production of RDOM mainly through regulation of hypolimnetic temperature. The positive shift of in situ production efficiency relative to the low temperature environment in the dark Japan Sea and Lake Biwa may be ascribed to high sinking fluxes of bio-labile materials in these temperate and often eutrophic aquatic systems (Kim et al., 2011; Thottathil et al., 2013). Thus, the downward supply of labile substrates to the hypolimnion undoubtedly alters the production of RDOM in the hypolimnion.

The lack of correlation between $FDOM_H$ and AOU makes it difficult to estimate the direct production of hypolimnetic RDOM during non-stratified periods. Alternatively, the net increase in the lateral $FDOM_H$ flux after reservoir regulation was used as a measure of net production. Although the WRTs of autumn and winter were quite long (31–49.6 days), there was low net production of $FDOM_H$ during the non-stratified autumn (0.04×10^9 RU m^3) and winter (0.11×10^9 RU m^3) (Table S3). This is consistent with the weak degradation of UA+Peptides with a high H/C ratio (> 1.5) (Fig. 6e-l). The low production potential of $FDOM_H$ in autumn may be attributed to restriction of microbial activity by oxygen limitation (DO < 2 ppm) resulting from the long WRT during this period (Fig. 2h). However, the low winter temperatures appeared to limit $FDOM_H$ production more than the oxygen-limited conditions in autumn (Fig. 2m). In contrast, the replenishment of DO and bio-labile DOM in winter primes the system for increased production of RDOM during the subsequent spring season when warmer temperatures and stratification develop.

4.3. Implications

4.3.1. Inland dark waters are hotspots for microbial RDOM production

Previous studies report that large RDOM pools are a by-product of microbial mineralization in the global dark ocean and marginal basins (Yamashita and Tanoue, 2008; Wang et al., 2021a). Investigations in the hypolimnion of inland reservoirs (SK, Hongjiadu and Three Gorges) and lakes (Biwa) further corroborate that deoxygenation-driven microbial RDOM production is a ubiquitous phenomenon in dark aquatic systems (Thottathil et al., 2013; Wang et al., 2021b; Yi et al., 2021). Combined with the finding of microbial RDOM accumulation in soil systems (Cai et al., 2022), this phenomenon could be the general mechanism of RDOM production in all natural ecosystems, including aquatic surface oxygenated layers. However, due to overlapping regulation of DOM and oxygen by complex physical and biogeochemical factors, quantifying the production rate for RDOM in surface layers remains a big challenge.

In SK reservoir, the net in situ production rate of hypolimnetic $FDOM_H$ in summer was significantly higher than in spring and early autumn ($p < 0.05$), with much faster turnover in the warmer summer season (Table 1). Surprisingly, these rates from inland systems are four

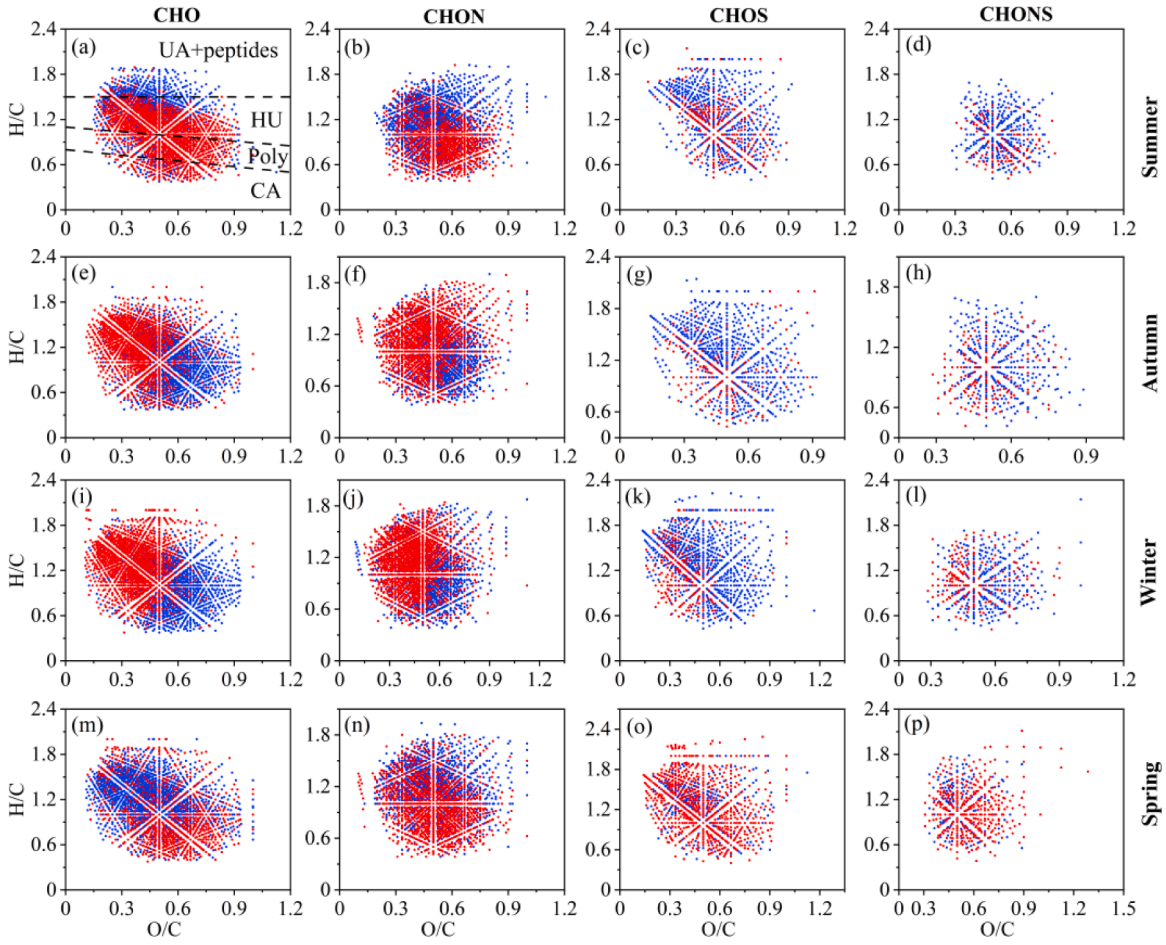

Fig. 6. Van Krevelen diagrams of molecular differences between the epilimnetic (surface) and hypolimnetic (bottom) DOM in different seasons during 2020–2021 as determine by FT-ICR MS analysis. A molecule was enriched if normalized peak abundance of hypolimnetic DOM was higher than of epilimnetic DOM (red points) and depleted if vice versa (blue points).

Table 1
Temperature, oxygen utilization rate (OUR), in situ production efficiency, rate and turnover time of $FDOM_H$ in inland waters and ocean systems. IW: Intermediate Water (200–1000 m); DW: Deep Water (>1000 m). The data from Lake Biwa (Japan), Three Gorges reservoir and ocean systems are from Thottathil et al. (2013), Wang et al. (2021b) and Wang et al. (2021a), respectively. Turnover times for $FDOM_H$ in 2017 and 2019 were unavailable due to lack of net production inventory data.

Region	Study area	Temperature (°C)	OUR (μmol kg^{-1} d^{-1})	*In situ* production efficiency of $FDOM_H$ (QSU (μmol L^{-1}) $^{-1}$)	*In situ* production rate of $FDOM_H$ (QSU d^{-1})	Turnover time
Inland waters	SK $Reservoir_{summer-2021}$	28.2 ± 1.8	12.1 ± 3.9	0.0151±0.0043	0.19±0.06	20.8 ± 6.6 d
	SK $Reservoir_{spring-2021}$	17.5 ± 2.6	6.6 ± 0.7	0.0054±0.0019	0.04±0.01	18.8 ± 2.0 d
	SK $Reservoir_{autumn-2019}$	29.5 ± 1.6	6.1 ± 1.4	0.0107±0.0035	0.07±0.02	—
	SK $Reservoir_{summer-2017}$	28.7 ± 1.3	13.3 ± 6.6	0.0111±0.0027	0.15±0.07	—
	Three Gorges Reservoir	21.2 ± 0.7	—	0.0147±0.0024	—	—
	Lake Biwa (Japan)	~8.2	—	0.0082	—	—
Ocean systems	South China Sea_{IW}	7.8 ± 0.4	(4.7 ± 2.0) × 10^{-3}	0.0034±0.0004	(1.6 ± 0.2) × 10^{-5}	186±78 yr
	South China Sea_{DW}	2.5 ± 0.1	(1.6 ± 0.2) × 10^{-3}	0.0030±0.0011	(0.5 ± 0.2) × 10^{-5}	647±249 yr
	Japan Sea_{IW}	0.7 ± 0.2	(14±0.3) × 10^{-3}	0.0040±0.0014	(5.6 ± 0.12) × 10^{-5}	91±32 yr
	West Med Sea_{IW}	13.3 ± 0.3	(1.7 ± 0.2) × 10^{-3}	0.0048±0.0016	(0.8 ± 0.2) × 10^{-5}	370±92 yr
	Global $Ocean_{IW}$	6.8 ± 0.3	(1.8 ± 0.1) × 10^{-3}	0.0034±0.0003	(0.6 ± 0.05) × 10^{-5}	538±167 yr

to five orders-of-magnitude higher than in ocean systems due to high in situ production efficiency and OUR (Table 1). Meanwhile, the turnover times for $FDOM_H$ (20 ± 4.2 days) in the dark hypolimnion are much shorter than in the global dark oceans (538 ± 367 year) due to short WRTs. These data clearly demonstrate that inland dark waters are hotspots of microbial RDOM production in aquatic systems.

4.3.2. *Hypolimnetic regulation of RDOM storage and export for inland waters*

Global reservoir and lake volumes are estimated as 8069 km^3 (Global Reservoirs and Dams database) and 181,900 km^3 (Messager et al., 2016), respectively. Recent studies documented widespread hypolimnetic deoxygenation in global reservoirs and lakes (Jane et al., 2021). Based on results from SK and several other reservoirs/lakes, we speculate that there could be a large storage of hypolimnetic RDOM in inland waters, especially for stratified lakes with longer WRTs. Continued global dam building is projected to increase allochthonous and autochthonous carbon substrates to inland waters (Maavara et al., 2017). The projected temperature increase under future global warming scenarios could enhance microbial utilization of these bio-labile DOM components and thus in situ production of RDOM in the hypolimnion of inland waters (Kraemer et al., 2015; van Vliet et al., 2011). Future studies of reservoirs/lakes from low to high latitudes are warranted to constrain this inland RDOM inventory and evaluate its role in aquatic carbon cycling.

There was a net increase of lateral $FDOM_H$ fluxes in the Min and Wujiang rivers after impoundment in the stratified SK (10.8–32.1%) and Hongjiadu (25.1%) reservoirs, respectively (Yi et al., 2021). This suggests that lateral delivery of the hypolimnetic RDOM pool could increase the recalcitrance of fluvial DOM by as much as 77% in global long rivers with reservoirs during periods of stratification (Grill et al., 2019). These RDOM components may finally be transported through the estuary into the sea changing coastal carbon cycling dynamics, if not photodegraded during transport. Furthermore, the lateral RDOM transport flux and its by-products (nutrients) could be intensified due to ongoing dam building, resulting in additional hypolimnetic DOM processing by global reservoirs. Thus, impoundment of rivers may represent a major anthropogenic modification of the carbon cycle altering both DOM quantity and quality along the river continuum and at the land-sea interface. The short WRT during the spring-flood event revealed that the hypolimnetic RDOM produced during the stratified period can be quickly flushed from reservoirs during flood events. This view of quickly increasing riverine $FDOM_H$ from reservoir releases at the onset of storm events is in contrast to the traditional view of soil DOM flushing/leaching processes dominating riverine DOM dynamics during storm events (Yang et al., 2013). In sum, this study highlights the importance of hypolimnetic production of RDOM in stratified reservoirs, and hence the need to consider hypolimnetic transformations in models simulating the fate and transport of carbon from inland waters across the land-sea interface.

5. Conclusions

This study provides compelling evidence (optical and molecular properties of DOM) that seasonal reservoir regulation changes the quality and quantity of DOM along the river-reservoir-river continuum. We found that the epilimnetic bio-labile DOM pool was largely contributed by algal blooms during the spring/summer, with baseflow providing additional bio-labile DOM during the spring. During periods of stratification (spring/summer), bio-refractory DOM (e.g., CRAMs) increased with depth in the hypolimnion and was accompanied by a simultaneous decrease of bio-labile DOM (e.g., aliphatic compounds and heteroatomic HU compounds containing N or S) and biogenic POM, which further showed a strong correlation with AOU. These findings demonstrates deoxygenation-enhanced production of RDOM during seasonal periods of thermal stratification. The efficiency and rate of hypolimnetic humic-like FDOM ($FDOM_H$) production were mainly regulated by temperature and availability of bio-labile substrates, and were significantly higher than those production parameters in dark ocean environments. Our study emphasized that inland dark waters are hotspots for microbial production of RDOM, which increases the recalcitrance of DOM along the land-to-sea continuum. Future studies are warranted to further explore the mechanisms controlling the interactions between microbial metabolism and DOM transformations under different oxygen availability conditions.

Declaration of Competing Interest

The authors declare that they have no known competing financial interests or personal relationships that could have appeared to influence the work reported in this paper.

Acknowledgments

This work was jointly supported by National Natural Science Foundation of China (41876083, 41276064) and State Key Laboratory of Heavy Oil Processing, China University of Petroleum - Beijing. Special thanks to Shuikou Hydropower Station for providing cruise vessel and Baoyi Feng and Qinglong Liang for their help in sampling. The authors thank Ms. Jing Xu, Dr. Qibiao Yu and Dr. Chao Wang for their help in data processing and visualization. The authors are grateful to Professors Si-liang Li and Ding He for kindly sharing data from Hongjiadu and Three Gorges reservoirs. We would like to thank the anonymous reviewers for their valuable comments and suggestions.

Supplementary materials

Supplementary material associated with this article can be found, in the online version, at doi:10.1016/j.watres.2022.118537.

References

Attermeyer, K., Catalan, N., Einarsdottir, K., Freixa, A., Groeneveld, M., Hawkes, J.A., et al., 2018. Organic carbon processing during transport through boreal inland waters: particles as important sites. J. Geophys. Res-Biogeosci. 123 (8), 2412–2428.
Bhattacharya, R., Osburn, C.L., 2020. Spatial patterns in dissolved organic matter composition controlled by watershed characteristics in a coastal river network: the Neuse River Basin, USA. Water Res. 169, 115248.
Cai, Y., Ma, T., Wang, Y., Jia, J., Jia, Y., Liang, C., et al., 2022. Assessing the accumulation efficiency of various microbial carbon components in soils of different minerals. Geoderma 407, 115562.
Catalá, T.S., Reche, I., Fuentes-Lema, A., Romera-Castillo, C., Nieto-Cid, M., Ortega-Retuerta, E., et al., 2015. Turnover time of fluorescent dissolved organic matter in the dark global ocean. Nat Commun. 6, 5986.
Chen, M.L., Kim, S.H., Jung, H.J., Hyun, J.H., Choi, J.H., Lee, H.J., et al., 2017. Dynamics of dissolved organic matter in riverine sediments affected by weir impoundments: production, benthic flux, and environmental implications. Water Res. 121, 150–161.
Cory, R.M., Harrold, K.H., Neilson, B.T., Kling, G.W., 2015. Controls on dissolved organic matter (DOM) degradation in a headwater stream: the influence of photochemical and hydrological conditions in determining light-limitation or substrate-limitation of photo-degradation. Biogeosciences 12 (22), 6669–6685.
Dittmar, T., Koch, B., Hertkorn, N., Kattner, G., 2008. A simple and efficient method for the solid-phase extraction of dissolved organic matter (SPE-DOM) from seawater. Limnol. Oceanogr. Methods 6, 230–235.
Flerus, R., Lechtenfeld, O.J., Koch, B.P., McCallister, S.L., Schmitt-Kopplin, P., Benner, R., et al., 2012. A molecular perspective on the ageing of marine dissolved organic matter. Biogeosciences 9 (6), 1935–1955.
Grill, G., Lehner, B., Thieme, M., Geenen, B., Tickner, D., Antonelli, F., et al., 2019. Mapping the world's free-flowing rivers. Nature 569 (7755), 215–221.
Guo, W.D., Yang, L.Y., Zhai, W.D., Chen, W.Z., Osburn, C.L., Huang, X., et al., 2014. Runoff-mediated seasonal oscillation in the dynamics of dissolved organic matter in different branches of a large bifurcated estuary-The Changjiang Estuary. J. Geophys. Res. Biogeosci. 119 (5), 776–793.
Han, Q., Wang, B.L., Liu, C.Q., Wang, F.S., Peng, X., Liu, X.L., 2018. Carbon biogeochemical cycle is enhanced by damming in a karst river. Sci. Total Environ. 616, 1181–1189.
Hansman, R.L., Dittmar, T., Herndl, G.J., 2015. Conservation of dissolved organic matter molecular composition during mixing of the deep water masses of the northeast Atlantic Ocean. Mar. Chem. 177, 288–297.

He, C., Zhang, Y., Li, Y., Zhuo, X., Li, Y., Zhang, C., et al., 2020a. In-house standard method for molecular characterization of dissolved organic matter by FT-ICR mass spectrometry. ACS Omega 5 (20), 11730–11736.
He, D., Wang, K., Pang, Y., He, C., Li, P.H., Li, Y.Y., et al., 2020b. Hydrological management constraints on the chemistry of dissolved organic matter in the Three Gorges Reservoir. Water Res. 187, 116413.
Hockaday, W.C., Purcell, J.M., Marshall, A.G., Baldock, J.A., Hatcher, P.G., 2009. Electrospray and photoionization mass spectrometry for the characterization of organic matter in natural waters: a qualitative assessment. Limnol. Oceanogr. Methods 7, 81–95.
Hong, H.S., Yang, L.Y., Guo, W.D., Wang, F.L., Yu, X.X., 2012. Characterization of dissolved organic matter under contrasting hydrologic regimes in a subtropical watershed using PARAFAC model. Biogeochemistry 109 (1–3), 163–174.
Huber, S.A., Balz, A., Abert, M., Pronk, W., 2011. Characterisation of aquatic humic and non-humic matter with size-exclusion chromatography-organic carbon detection-organic nitrogen detection (LC-OCD-OND). Water Res. 45 (2), 879–885.
Jane, S.F., Hansen, G.J.A., Kraemer, B.M., Leavitt, P.R., Mincer, J.L., North, R.L., et al., 2021. Widespread deoxygenation of temperate lakes. Nature 594 (7861), 66–70.
Jiao, N.Z., Cai, R.H., Zheng, Q., Tang, K., Liu, J.H., Jiao, F.L.E., et al., 2018. Unveiling the enigma of refractory carbon in the ocean. Natl. Sci. Rev. 5 (4), 459–463.
Kellerman, A.M., Guillemette, F., Podgorski, D.C., Aiken, G.R., Butler, K.D., Spencer, R.G. M., 2018. Unifying concepts linking dissolved organic matter composition to persistence in aquatic ecosystems. Environ. Sci. Technol. 52 (5), 2538–2548.
Kim, D., Choi, M.-.S., Oh, H.-.Y., Song, Y.-.H., Noh, J.-.H., Kim, K.H., 2011. Seasonal export fluxes of particulate organic carbon from $^{234}Th/^{238}U$ disequilibrium measurements in the Ulleung Basin (Tsushima Basin) of the East Sea (Sea of Japan). J. Oceanogr. 67 (5), 577–588.
Koch, B.P., Dittmar, T., 2016. From mass to structure: an aromaticity index for high-resolution mass data of natural organic matter. Rapid Commun. Mass Sp 30 (1), 250-250.
Kraemer, B.M., Anneville, O., Chandra, S., Dix, M., Kuusisto, E., Livingstone, D.M., et al., 2015. Morphometry and average temperature affect lake stratification responses to climate change. Geophys. Res. Lett. 42 (12), 4981–4988.
Lee, M.H., Osburn, C.L., Shin, K.H., Hur, J., 2018. New insight into the applicability of spectroscopic indices for dissolved organic matter (DOM) source discrimination in aquatic systems affected by biogeochemical processes. Water Res. 147, 164–176.
Liu, Y.Y., Wang, X.Y., Wang, Y.W., Tong, C., Yuan, W.P., 2019. Increased lateral transfer of soil organic carbon induced by climate and vegetation changes over the southeast coastal region of China. J. Geophys. Res. Biogeosci. 124 (12), 3902–3915.
Maavara, T., Lauerwald, R., Regnier, P., Van Cappellen, P., 2017. Global perturbation of organic carbon cycling by river damming. Nat. Commun. 8, 15347.
Mao, R., Li, S.Y., 2018. Temperature sensitivity of biodegradable dissolved organic carbon increases with elevating humification degree in subtropical rivers. Sci. Total Environ. 635, 1367–1371.
Martínez-Pérez, A.M., Osterholz, H., Nieto-Cid, M., Alvarez, M., Dittmar, T., Alvarez-Salgado, X.A., 2017. Molecular composition of dissolved organic matter in the Mediterranean Sea. Limnol. Oceanogr. 62, 2699–2712.
Messager, M.L., Lehner, B., Grill, G., Nedeva, I., Schmitt, O., 2016. Estimating the volume and age of water stored in global lakes using a geo-statistical approach. Nat. Commun. 7, 13603.
Oliver, A.A., Spencer, R.G.M., Deas, M.L., Dahlgren, R.A., 2016. Impact of seasonality and anthropogenic impoundments on dissolved organic matter dynamics in the Klamath River (Oregon/California, USA). J. Geophys. Res. Biogeosci. 121 (7), 1946–1958.
Ogawa, H., Amagai, Y., Koike, I., Kaiser, K., Benner, R., 2001. Production of refractory dissolved organic matter by bacteria. Science 292 (5518), 917–920.
Osterholz, H., Kilgour, D.P.A., Storey, D.S., Lavik, G., Ferdelman, T.G., Niggemann, J., et al., 2021. Accumulation of DOC in the South Pacific Subtropical Gyre from a molecular perspective. Mar. Chem. 231, 103955.
Pereira, R., Bovolo, C.I., Spencer, R.G.M., Hernes, P.J., Tipping, E., Vieth-Hillebrand, A., et al., 2014. Mobilization of optically invisible dissolved organic matter in response to rainstorm events in a tropical forest headwater river. Geophys. Res. Lett. 41 (4), 1202–1208.
Qu, L.Y., Jiao, T., Guo, W.D., Dahlgren, R.A., Ling, N., Feng, B.Y., 2021. Hydro-biogeochemical alterations to optical properties of particulate organic matter in the Changjiang Estuary and adjacent shelf area. Ecol. Indic. 128, 107837.
Raymond, P.A., Spencer, R.G.M., 2015. Biogeochemistry of Marine Dissolved Organic Matter. Riverine DOM. In: Hansell Carlson (eds.), 2nd Edition. Academic Press, Boston, pp. 509–533.
Smale, D.A., Taylor, J.D., Coombs, S.H., Moore, G., Cunliffe, M., 2017. Community responses to seawater warming are conserved across diverse biological groupings and taxonomic resolutions. Proc. R. Soc. B-Biol. Sci. 284 (1862), 20170534.
Spencer, R.G.M., Aiken, G.R., Dornblaser, M.M., Butler, K.D., Holmes, R.M., Fiske, G., et al., 2013. Chromophoric dissolved organic matter export from U.S. rivers. Geophys. Res. Lett. 40 (8), 1575–1579.
Stedmon, C.A., Bro, R., 2008. Characterizing dissolved organic matter fluorescence with parallel factor analysis: a tutorial. Limnol. Oceanogr. Methods 6, 572–579.
Stubbins, A., Spencer, R.G.M., Chen, H., Hatcher, P.G., Mopper, K., Hernes, P.J., et al., 2010. Illuminated darkness: molecular signatures of Congo River dissolved organic matter and its photochemical alteration as revealed by ultrahigh precision mass spectrometry. Limnol. Oceanogr. 55 (4), 1467–1477.
Thottathil, S.D., Hayakawa, K., Hodoki, Y., Yoshimizu, C., Kobayashi, Y., Nakano, S., 2013. Biogeochemical control on fluorescent dissolved organic matter dynamics in a large freshwater lake (Lake Biwa, Japan). Limnol. Oceanogr. 58 (6), 2262–2278.
Van Vliet, M.T.H., Ludwig, F., Zwolsman, J.J.G., Weedon, G.P., Kabat, P., 2011. Global river temperatures and sensitivity to atmospheric warming and changes in river flow. Water Resour. Res. 47 (2), W02544.
Wagner, S., Dittmar, T., Jaffé, R., 2015. Molecular characterization of dissolved black nitrogen via electrospray ionization Fourier transform ion cyclotron resonance mass spectrometry. Org. Geochem. 79, 21–30.
Wagner, S., Fair, J.H., Matt, S., Hosen, J.D., Raymond, P., Saiers, J., et al., 2019. Molecular hysteresis: hydrologically driven changes in riverine dissolved organic matter chemistry during a storm event. J. Geophys. Res. Biogeosci. 124 (4), 759–774.
Wang, C., Guo, W., Li, Y., Dahlgren, R.A., Guo, X., Qu, L., et al., 2021a. Temperature-regulated turnover of chromophoric dissolved organic matter in global dark marginal basins. Geophys. Res. Lett. 48 (19) e2021GL094035.
Wang, K., Li, P., He, C., Shi, Q., He, D., 2021b. Density currents affect the vertical evolution of dissolved organic matter chemistry in a large tributary of the Three Gorges Reservoir during the water-level rising period. Water Res. 204, 117609.
Xu, H., Yan, M., Long, L.H., Ma, J., Ji, D.B., Liu, D.F., et al., 2021. Modeling the effects of hydrodynamics on thermal stratification and algal blooms in the Xiangxi Bay of Three Gorges Reservoir. Front. Ecol. Evol. 8, 610622.
Yamashita, Y., Tanoue, E., 2008. Production of bio-refractory fluorescent dissolved organic matter in the ocean interior. Nat. Geosci. 1 (9), 579–582.
Yan, J., Chen, N., Wang, F., Liu, Q., Wu, Z., Middelburg, J.J., et al., 2021. Interaction between oxygen consumption and carbon dioxide emission in a subtropical hypoxic reservoir, Southeastern China. J. Geophys. Res. Biogeosci. 126 (4) e2020JG006133.
Yang, L.Y., Choi, J.H., Hur, J., 2014. Benthic flux of dissolved organic matter from lake sediment at different redox conditions and the possible effects of biogeochemical processes. Water Res. 61, 97–107.
Yang, L.Y., Guo, W.D., Chen, N.W., Hong, H.S., Huang, J.L., Xu, J., et al., 2013. Influence of a summer storm event on the flux and composition of dissolved organic matter in a subtropical river, China. Appl. Geochem. 28, 164–171.
Yi, Y.B., Zhong, J., Bao, H.Y., Mostofa, K.M.G., Xu, S., Xiao, H.Y., et al., 2021. The impacts of reservoirs on the sources and transport of riverine organic carbon in the karst area: a multi-tracer study. Water Res. 194, 116993.
Yu, L.Q., Gan, J.P., Dai, M.H., Hui, C.R., Lu, Z.M., Li, D., 2021. Modeling the role of riverine organic matter in hypoxia formation within the coastal transition zone off the Pearl River Estuary. Limnol. Oceanogr. 66 (2), 452–468.
Regnier, P., Resplandy, L., Najjar, R.G., Ciais, P., 2022. The land-to-ocean loops of the global carbon cycle. Nature 603 (7901), 401–410.
Zhou, L., Zhou, Y.Q., Tang, X.M., Zhang, Y.L., Jang, K.S., Szekely, A.J., et al., 2021. Resource aromaticity affects bacterial community successions in response to different sources of dissolved organic matter. Water Res. 190, 116776.
Zhou, Y.P., Zhao, C., He, C., Li, P.H., Wang, Y.T., Pang, Y., et al., 2022. Characterization of dissolved organic matter processing between surface sediment porewater and overlying bottom water in the Yangtze River Estuary. Water Res. 215, 118260.